THS



This is to certify that the

thesis entitled

THE PREPARATION AND STRUCTURE

CHARACTERIZATION OF Sm<sub>5</sub>YBr<sub>13</sub>

presented by

Paul Anthony Pezzoli

has been accepted towards fulfillment of the requirements for

M.S. degree in Chemistry

Major professor

Date 10 . 17, 1977

**O**-7639

# THE PREPARATION AND STRUCTURE CHARACTERIZATION OF $sm_5 yBr_{13}$

By

Paul Anthony Pezzoli

#### A THESIS

Sumbitted to

Michigan State University

in partial fulfillment of the requirements

for the degree of

MASTER OF SCIENCE

Department of Chemistry

#### **ABSTRACT**

# THE PREPARATION AND STRUCTURE CHARACTERIZATION OF $sm_5 y Br_{13}$

By

#### Paul Anthony Pezzoli

A unique compound,  $\mathrm{Sm}_5\mathrm{YBr}_{13}$ , was prepared upon the reaction of samarium metal with samarium tribromide and yttrium tribromide. This samarium yttrium bromide phase was identified and characterized by analytical techniques and X-ray diffractometry. The gray-black product was found to exhibit monoclinic symmetry. The space group for this compound is C2/c. Unit cell lattice parameters calculated by least squares regression analysis are:  $\underline{a} = 44.31_0 \pm 0.05_1 \, \mathring{A}, \, \underline{b} = 7.139_4 \pm 0.008_2 \, \mathring{A}, \, \underline{c} = 7.651_1 \pm 0.007_5 \, \mathring{A}$  and angle  $\underline{\beta} = 98.45_1 \pm 0.06_8 \, \mathring{C}$ . This phase was identified as a member of a class of compounds of the general formula  $\mathrm{Mn}_{\mathrm{N}}\mathrm{Mn}_{\mathrm{N}}\mathrm{Mn}_{\mathrm{N}}$  where n=6, which exhibit a vernier-type structure. Single crystals of  $\mathrm{Sm}_5\mathrm{YBr}_{13}$  were prepared for future structural analysis.

Attempts to prepare the hafnium analog,  $Sm_5HfBr_{13}$ , were unsuccessful.

#### ACKNOWLEDGEMENTS

The author wishes to express sincere appreciation to Professor Harry A. Eick for the guidance, patience and assistance he provided during the course of this research.

My parents are acknowledged, in particular for their encouragement and hopes in the attainment of this educational goal.

The members of the High Temperature Group are acknowledged for their help and fruitful discussions.

Appreciation is extended to Lisa Ittner, who spent many long hours typing this manuscript.

Finally, the financial and moral support of The Dow Chemical Company and, in particular the management of the Central Research Inorganic Laboratory, is most gratefully acknowledged.

# TABLE OF CONTENTS

Chapter		Page
I	INTRODUCTION	1
II	BACKGROUND AND THEORETICAL CONSIDERATIONS.	4
	PREPARATION OF RARE EARTH HALIDES	5
	Rare Earth Trihalides	5
	Rare Earth Dihalides	6
	Single Crystal Preparation	7
	Mixed Valence Rare Earth Halides	7
	STRUCTURAL INFORMATION	8
	Samarium Tribromide	8
	A. Anhydrous Samarium Tribromide	10
	B. Samarium Tribromide Hexahydrate .	10
	Samarium Dibromide	10
	A. Anhydrous Samarium Dibromide	10
	B. Samarium Dibromide Monohydrate	10
	Mixed Valence Samarium Bromide	11
	Yttrium Tribromide	11
	Hafnium Tetrabromide	11
III	EXPERIMENTAL PROCEDURES	14
	CHEMICALS AND MATERIALS	15
	HANDLING PROCEDURES	15

Chapter		Page
	PREPARATIVE PROCEDURES	15
	Anhydrous Samarium Tribromide	15
	Reduced and Mixed Valence Samarium Bromides	18
	A. Sealed Containers	18
	1. Samarium Dibromide	18
	2. Sm <sub>6</sub> Br <sub>13</sub>	1,8
	3. $Sm_5YBr_{13}$	19
	4. Sm <sub>5</sub> HfBr <sub>13</sub>	19
	B. Open Containers	20
	1. Samarium Dibromide	20
	2. Sm <sub>6</sub> Br <sub>13</sub>	21
	3. Sm <sub>5</sub> YBr <sub>13</sub>	21
	4. Sm <sub>5</sub> HfBr <sub>13</sub>	21
	Samarium Tribromide Hexahydrate	22
	Samarium Dibromide Monohydrate	22
	Yttrium Tribromide	22
	Single Crystal Preparation	23
	ELEMENTAL ANALYSES	23
	Samarium Oxide Bromide	23
	Metal Analyses	24
	A. Conversion to Oxide	24
	B. Atomic Absorption Spectroscopy .	24
	Bromide Analyses	25
	A. Volhard Titration	25
	B. Atomic Absorption Spectroscopy .	26

	0h		<b>D</b>
,	Chapter		Page
		X-RAY POWDER DIFFRACTION PATTERNS	26
	IV	RESULTS	28
		ELEMENTAL ANALYSES	29
		X-RAY POWDER DIFFRACTION ANALYSES	29
		CALCULATION OF LATTICE PARAMETERS	31
		SINGLE CRYSTAL PREPARATION	36
	V <sub>.</sub>	DISCUSSION	37
	VI	CONCLUSION	46
	REFERENC	ES	49
	ADDENDIC	FS	53

## LIST OF TABLES

Table		Page
I	Metal Halide Compositions Defined by the Series ${}^M_n{}^X_{2n+1}$	9
II	Structural Information on the Samarium Bromides	12
III	Analytical Results of Several Samarium Bromide Phases	30
IV	Properties of Space Group C2/c	32
V	Data on Sm <sub>5</sub> YBr <sub>13</sub>	34
VI	Comparison of Lattice Parameters of $\mathrm{Sm_6^{Br}_{13}}$ and $\mathrm{Sm_5^{YBr}_{13}}$	35

# LIST OF FIGURES

Figure		Page
1	The Vernier Structures of Sm <sub>5</sub> Br <sub>11</sub> , Sm <sub>11</sub> Br <sub>24</sub> and Sm <sub>6</sub> Br <sub>13</sub> (As Outlined in Table II)	13
2	Samarium Bromide Preparation Apparatus .	17
3	Representation of Space Group C2/c	33
4	Projection of $M_6X_{13}$ on (001) (Space Group I2/a)	41
5	Metal Atom Coordination in the $^{M}6^{X}13$ Lattice	43

### LIST OF APPENDICES

Appendix		Page
Α	The Positional and Thermal Parameters of SmBr <sub>2</sub>	53
В	The Positional and Thermal Parameters of Sm <sub>5</sub> Br <sub>11</sub>	54
С	The Positional and Thermal Parameters of Sm <sub>6</sub> Br <sub>13</sub> and Sm <sub>5</sub> YBr <sub>13</sub>	55
D	X-Ray Powder Diffraction Pattern of Tetragonal SmBr <sub>2</sub>	56
E	X-Ray Powder Diffraction Pattern of Orthorhombic SmBr <sub>2</sub> ·H <sub>2</sub> O	57
F	X-Ray Powder Diffraction Pattern of Orthorhombic SmBr <sub>3</sub>	58
G	X-Ray Powder Diffraction Pattern of Monoclinic SmBr <sub>3</sub> ·6H <sub>2</sub> O	59
Н	X-Ray Powder Diffraction Pattern of of Tetragonal SmOBr	61
I .	X-Ray Powder Diffraction Pattern of Vernier Sm <sub>5</sub> Br <sub>11</sub>	62
J	X-Ray Powder Diffraction Pattern of Vernier Sm <sub>6</sub> Br <sub>13</sub>	64
K	X-Ray Powder Diffraction Pattern of Monoclinic YBr <sub>3</sub>	66
L	X-Ray Powder Diffraction Pattern of Vernier Sm <sub>5</sub> YBr <sub>13</sub>	67
М	X-Ray Powder Diffraction Pattern of Cubic HfBr <sub>4</sub>	69
N	Least Squares Refinement of Sm <sub>5</sub> YBr <sub>13</sub>	70

CHAPTER I INTRODUCTION

#### INTRODUCTION

During the past decade the preparation and characterization of lower valence and mixed valence compounds have received considerable attention. Much of the research effort has been concentrated in the area of the rare earth halides. Stable reduced valence metal halides have been studied extensively and are reviewed by Corbett.  $^{1,2}$  Many systems studied recently can be defined by a homologous series  $^{\rm M}{}_{\rm N} ^{\rm X}{}_{\rm 2n+1}$  where M is a rare earth metal and X is a halide. Compounds in the series exhibit a complex verniertype structure.

Several of the mixed valence rare earth halides have been characterized and their structures determined by single crystal X-ray structure analysis. Others have been prepared as polycrystalline phases and the resultant structures determined from powder diffraction patterns. One such system is the SmBr<sub>X</sub> system which has been studied in detail by Haschke. He could not isolate single crystals of the compounds.

The inability to prepare single crystals of  ${\rm Yb_6Cl_{13}}$  was reported by Lüke and Eick. Single crystals of the desired structure were obtained only after  ${\rm Er}^{3+}$  was partially substituted for  ${\rm Yb}^{3+}$  in the preparation. Erbium was chosen for the system because its ionic radius was similar to that of ytterbium.

The objective of this work was to study further the  ${\rm SmBr}_{\rm x}$  system, and more specifically the compound  ${\rm Sm}_6{\rm Br}_{13}$ . As in the  ${\rm YbCl}_{\rm x}$  system, it was thought possible to prepare and isolate single crystals of this structure if another ion of similar ionic radius was substituted for samarium in the lattice. Substitution of a transition metal into the lattice of a rare earth halide could result in the determination of the site symmetry of the trivalent and divalent metal ions since the electron density of a first or second row transition metal is significantly less than that of a rare earth metal. The metals used in this investigation were yttrium and hafnium. Attempts were made to prepare the compounds  ${\rm Sm}_5{\rm YBr}_{13}$  and  ${\rm Sm}_5{\rm HfBr}_{13}$ . X-Ray powder diffraction analysis was used to determine if these compounds exhibited the same structure as  ${\rm Sm}_6{\rm Br}_{13}$ .

# CHAPTER II BACKGROUND AND THEORETICAL CONSIDERATIONS

## PREPARATION OF RARE EARTH HALIDES

#### Rare Earth Trihalides

Aqueous solutions of rare earth trihalides can be readily prepared. However, only highly hydrated products separate from these solutions (usually six moles of bound water). Most of the water can be removed through dehydration at low temperatures but the last mole is difficult to remove without decomposing the halide to the oxide halide.

In the past few years many methods have been developed to produce relatively pure anhydrous rare earth trihalides. Most of the preparative procedures involve the trichlorides. Matignon 6 first described the preparation of rare earth trichlorides by dehydration of the hydrated trichloride with The method is described in detail by Taylor. There has also been extensive work done on the conversion of rare earth oxides to trihalides. The general method for chlorination of oxides with S2Cl2 and Cl2 was first reported near the turn of the century. 8 A modification of the same procedure involves the use of thionyl chloride. 9, 10 Carbon tetrachloride 11 and phosgene 12 have also been used to convert rare earth oxides to trichlorides. Other rare earth trichloride preparative procedures are outlined by Taylor. 7 The chlorination of rare earth oxides with ammonium chloride is reported by Domning and Schechter. 13 High purity trichlorides also have been prepared from the reaction of a rare earth oxide and various amine hydrochlorides. 14

Fewer methods have been perfected for preparing anhydrous rare earth tribromides than exist for preparation of the trichlorides. Borisov et al. 15 prepared several rare earth tribromides by reaction of the oxide with carbon and bromine. While most of the procedures outlined above for the preparation of the trichlorides can be adapted for the preparation of the tribromides, the most successful and widely used one is that described by Taylor and Carter. 16 The procedure involves careful dehydration of the hydrated tribromide in the presence of an excess of ammonium bromide. Because of its acidic nature, the excess ammonium bromide is believed to prevent hydrolysis of the rare earth tribromide. Haschke and Eick 17 extensively studied the europium bromide system using a modification of the Taylor-Carter process. Rare earth tribromides can also be prepared from the reaction of a rare earth metal and an excess amount of mercuric bromide at elevated temperatures. 18

#### Rare Earth Dihalides

Most of the work involving rare earth dihalides has been done in the past twenty years. As in the case of the trihalides, the dichlorides have received the most attention. Polyachenok and Novikov<sup>19</sup> studied the thermodynamics of the reaction

$$3MCl2(s) - 2MCl3(s) + M(s)$$
 (1)

Their calculations showed that many rare earth dichlorides exist only in a metastable state.

Many ways have been used to reduce rare earth trihalides to the dihalides. One method involves reduction of the trihalide by hydrogen. Another technique, reported by DeKock and Radtke, uses zinc as a reducing agent in a zinc chloride melt. Whenever the dihalide is only slightly stable toward disproportionation the metal of the cation involved is the most obvious and suitable reducing agent. The procedure for the reaction

$$2MX_3(1) + M(s,1) - 3MX_2(1)$$
 (2)

where X = Cl, Br, I has been outlined by Corbett.<sup>2</sup>

# Single Crystal Preparation

The preparation and growth of single crystals of rare earth halides have been described by Cox and Fong<sup>22</sup> and Mroczkowski.<sup>23</sup> These techniques involve very slow cooling of a liquid melt.

# Mixed Valence Rare Earth Halides

The preparation and characterization of rare earth dihalides and mixed valence halide compositions have been widely reported recently. Mixed valence rare earth halides have been prepared either by reaction of the metal with the trihalide or reaction of the trihalide with the dihalide. The compounds were isolated from a melt which was contained in reaction vessels of tantalum, gold, carbon or quartz. Corbett and co-workers have done extensive work on

the systems  ${\rm MX}_{\leq 1.5}$ , which exhibit a high degree of metalmetal bonding. The compounds  ${\rm Gd_2Cl_3}$ ,  $^{24}$   ${\rm Sc_2Cl_3}$  and  ${\rm Sc_2Br}$ ,  $^{25}$   ${\rm Sc_7Cl_{10}}^2$  and  ${\rm ScCl}^{27}$  have been isolated. The monochlorides of gadolinium and terbium have also been prepared.  $^{28}$  The crystal structures of the rare earth monochlorides are sheet-like and are similar to the phases reported for  ${\rm ZrBr}^{29}$  and  ${\rm HfCl.}^{30}$ 

Some mixed valence halides exhibit vernier-type structures. Such structures were reviewed by Hyde et al.  $^{31}$  and were identified as the crystal structure for the compounds  $^{4}7^{0}6^{F}9$ ,  $^{32}$  Nb $_{2}^{2}r_{6}^{0}17$  and  $^{33}$  and  $^{2}r_{10}8^{N}98^{F}138$ .

An examination of the reported intermediate valence phases shows that some compositions are consistent with an  $M_n X_{2n+2}$  series. Reported compounds in this series include  $Sm_{11}Br_{24}$ ,  $^4$  La $_5I_{12}$ ,  $^{35}$  Pr $_5Br_{12}$  and Yb $_6Cl_{14}$ .

Mixed valence rare earth halides also exist as compounds which can be assigned to the homologous series  $M_n X_{2n+1}$ . The compounds in this series which have been isolated and characterized are listed in Table I. Mixed-metal rare earth halides that also belong to this series have been reported. They are  $Sr_4DyCl_{11}^3$  and  $Yb_5ErCl_{13}^5$  where n = 5 and 6 respectively.

#### STRUCTURAL INFORMATION

#### Samarium Tribromide

# A. Anhydrous Samarium Tribromide

Anhydrous samarium tribromide exists in the PuBr3-type

TABLE I: Metal Halide Compositions Defined by the Series  ${\rm M}_n{\rm X}_{2n+1}$ 

	Theoretical		
n	X:M	Reported Compositions	Ref.
3	2.333	NdCl <sub>2.33</sub> , PrCl <sub>2.31</sub> , SmF <sub>2.35</sub>	39, 40, 41
4	2.250	NdCl <sub>2.25</sub> , NdCl <sub>2.27</sub> , YbCl <sub>2.26</sub>	38, 39, 40
5	2.200	SmBr <sub>2.20</sub> , NdCl <sub>2.20</sub> , SmCl <sub>2.20</sub> ,	4, 39, 43
		DyCl <sub>2.20</sub> , HoCl <sub>2.20</sub>	43, 44
6	2.167	SmBr <sub>2.172</sub>	4
9	2.111	DyCl <sub>2.11</sub> , TmCl <sub>2.11</sub>	45, 46
10	2.100	TmC12.10	46
11	2.091	TmCl <sub>2.090</sub>	46
12	2.080	TmC12.080	46
13	2.077	TmCl <sub>2.074</sub>	46
15	2.067	TmCl <sub>2.067</sub>	46
25	2.040	TmCl <sub>2.040</sub>	46

structure and is isostructural with NdBr<sub>3</sub>, EuBr<sub>3</sub> and TbBr<sub>3</sub>. The compound exhibits orthorhombic symmetry and is consistent with space group Ccmm.

## B. Samarium Tribromide Hexahydrate

Samarium tribromide hexahydrate is isostructural with the  $NdCl_3 \cdot 6H_2O$ -type structure<sup>48</sup> and the other rare earth tribromide hexahydrates.<sup>49</sup> The compound exhibits monoclinic symmetry and is consistent with space group P2/n.

### Samarium Dibromide

# A. Anhydrous Samarium Dibromide

Anhydrous samarium dibromide is isostructural with europium dibromide which exhibits X-ray patterns that are assignable to a tetragonal  $SrBr_2$ -type structure. 4 Systematic extinctions are consistent with space group P4/n.

# B. Samarium Dibromide Monohydrate

Samarium dibromide monohydrate, which exhibits a structure similar to that of EuBr<sub>2</sub>·H<sub>2</sub>O, <sup>17</sup> has not been prepared in pure form. X-Ray data for the compound assigns it to space group Pnma with an orthorhombic BaCl<sub>2</sub>·H<sub>2</sub>O-type structure. <sup>4</sup>

#### Mixed Valence Samarium Bromides

The three compositions isolated in the  $SmBr_{x}$  system all exhibit a vernier-type structure with monoclinic symmetry. Conditions for extinction show that  $Sm_5Br_{11}$  and  $Sm_{11}Br_{24}$  are assignable to space group P2. To facilitate comparison of the structure with that of  $Sm_5Br_{11}$ ,  $Sm_6Br_{13}$  has been indexed in space group I2/a.

Structural information for the various samarium bromide phases is detailed in Table II. The vernier structures of the samarium bromide phases as deduced by Bärnighausen<sup>3</sup> are shown in Figure 1. Vernier structures are layered structures with two metal atom layers (the open and filled circles) and two anion layers (the solid and broken line networks).

## Yttrium Tribromide

Yttrium tribromide is isostructural with  $AlCl_3$  and  $YCl_3$ . X-Ray data shows the compound to be of monoclinic symmetry and is indexable in the space group C2/m.

# Hafnium Tetrabromide

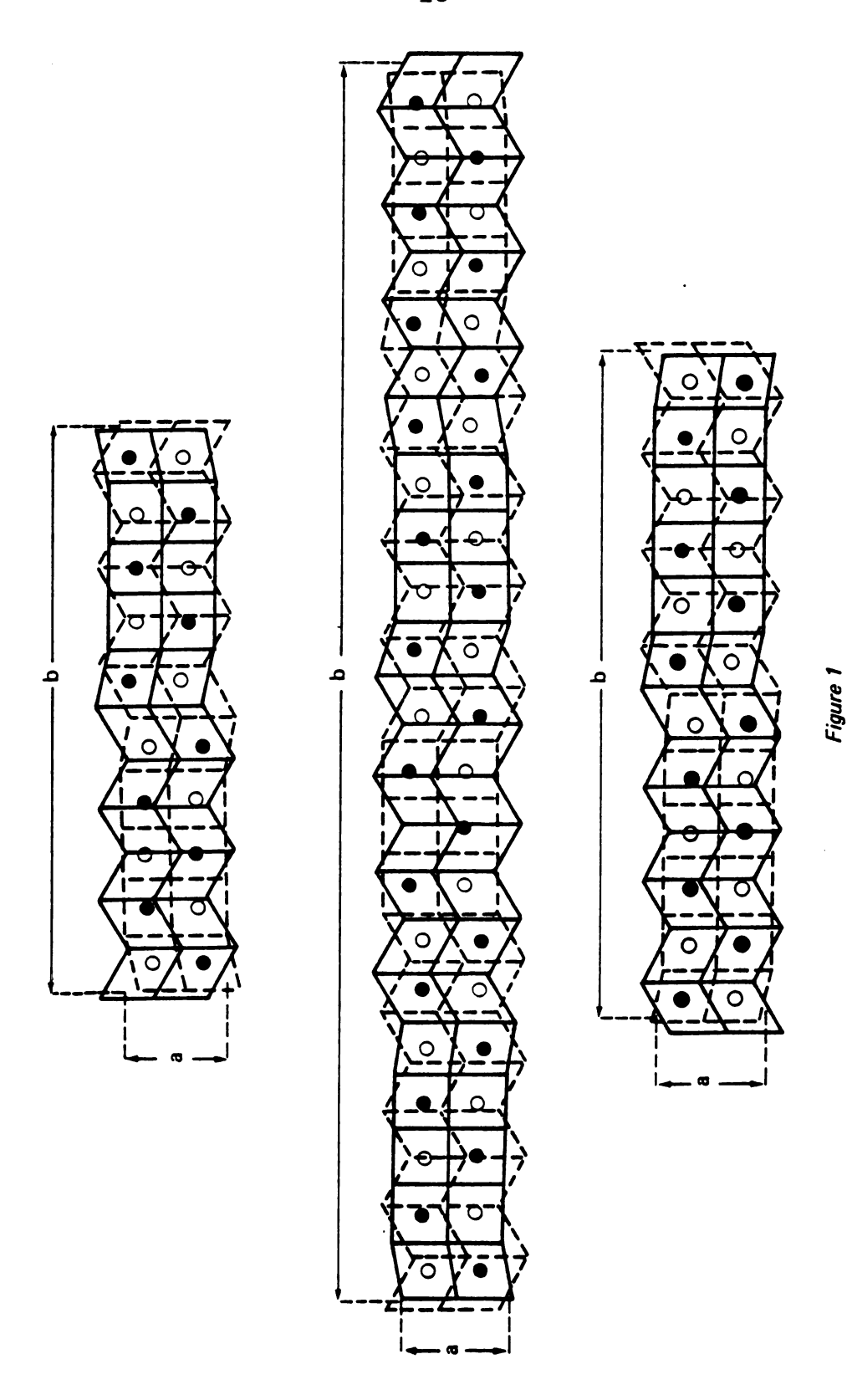
Hafnium tetrabromide exhibits cubic symmetry.

Systematic extinctions are consistent with space group

Pa3.

Structural Information on the Samarium Bromides TABLE II:

Species	Structure	Symmetry	Space Group	a (A)	b (Å)	c (Å)	β,γ(°)	Ref.
$SmBr_3$	PuBr <sub>3</sub>	orthorhmobic	Ccmm	4.042	12.706	9.124		47
$\mathrm{SmBr}_3 \cdot 6\mathrm{H}_2\mathrm{O}$	$^{\mathrm{NdCl}_3 \cdot 6\mathrm{H}_2\mathrm{O}}$	monoclinic	P2/n	10.03	6.762	8.158	93.57(8)	4
$\mathrm{SmBr}_2$	$SrBr_2$	tetragonal	P4/n	11.588		7.100		4
$\mathrm{SmBr}_2\cdot\mathrm{H}_2\mathrm{O}$	$BaCl_2 \cdot H_2O$	orthorhombic	Pnma	9.178	11.427	4.315		4
$Sm_5Br_{11}$	Vernier	monoclinic	P2/m	7.652	37.21	7.121	90.26(8)	က
$Sm_{11}Br_{24}$	Vernier	monoclinic	P2/n	7.652	81.62	7.130	90.19(8)	Э
$\mathrm{Sm}_{6}\mathrm{Br}_{13}$	Vernier	monoclinic	12/a .	7.649	44.44	7.139	91.30(y)	e
$\mathrm{Sm_5^{YBr}}_{13}$	Vernier	monoclinic	12/a	7.651	44.78	7.139	91.18(y)	This Work



From Top to Bottom: The Vernier Structures of Sm<sub>5</sub> Br<sub>11</sub>, Sm<sub>11</sub> Br<sub>24</sub> and Sm<sub>6</sub> Br<sub>13</sub> (As Outlined in Table II)

# CHAPTER III EXPERIMENTAL PROCEDURES

#### CHEMICALS AND MATERIALS

The chemicals and materials used were: (a) samarium oxide and yttrium oxide, 99.9%, Michigan Chemical Corp., St. Louis, MI; (b) samarium metal, samarium bromide, yttrium bromide, 99.9% and hafnium bromide, 98%, Cerac/Pure Chemical Co., Milwaukee, WI; (c) hydrobromic acid, 48% aqueous solution, Fisher Scientific Co., Fair Lawn, NJ; (d) ammonium bromide and ferric ammonium sulfate, reagent grade, Matheson, Coleman and Bell Chemical Co., Norwood, OH; (e) silver nitrate and potassium thiocyanate, reagent grade, J. T. Baker Chemical Co., Phillipsburg, NJ: (f) argon, Air Reduction Co., New York, NY; (g) vitreous carbon combustion boats, Beckwith Carbon Co., Van Nuys, CA; and (h) quartz tubing, Corning Glass Works, Corning, NY.

#### HANDLING PROCEDURES

The handling and storage of air and moisture sensitive materials such as SmBr<sub>3</sub>, YBr<sub>3</sub>, Sm, HfBr<sub>4</sub>, and the mixed valence bromides were performed in a recirculating argonatmosphere glove box. Hariharan<sup>50</sup> has described the glove box in detail. All weighings were done in the glove box. Samples were transported outside the glove box in evacuated Schlenk tubes or protected by a covering of Parafilm<sup>®</sup>M.

### PREPARATIVE PROCEDURES

Anhydrous Samarium Tribromide

Samarium tribromide was prepared according to a

modification of the method of Taylor and Carter. 16 The overall reaction is as follows:

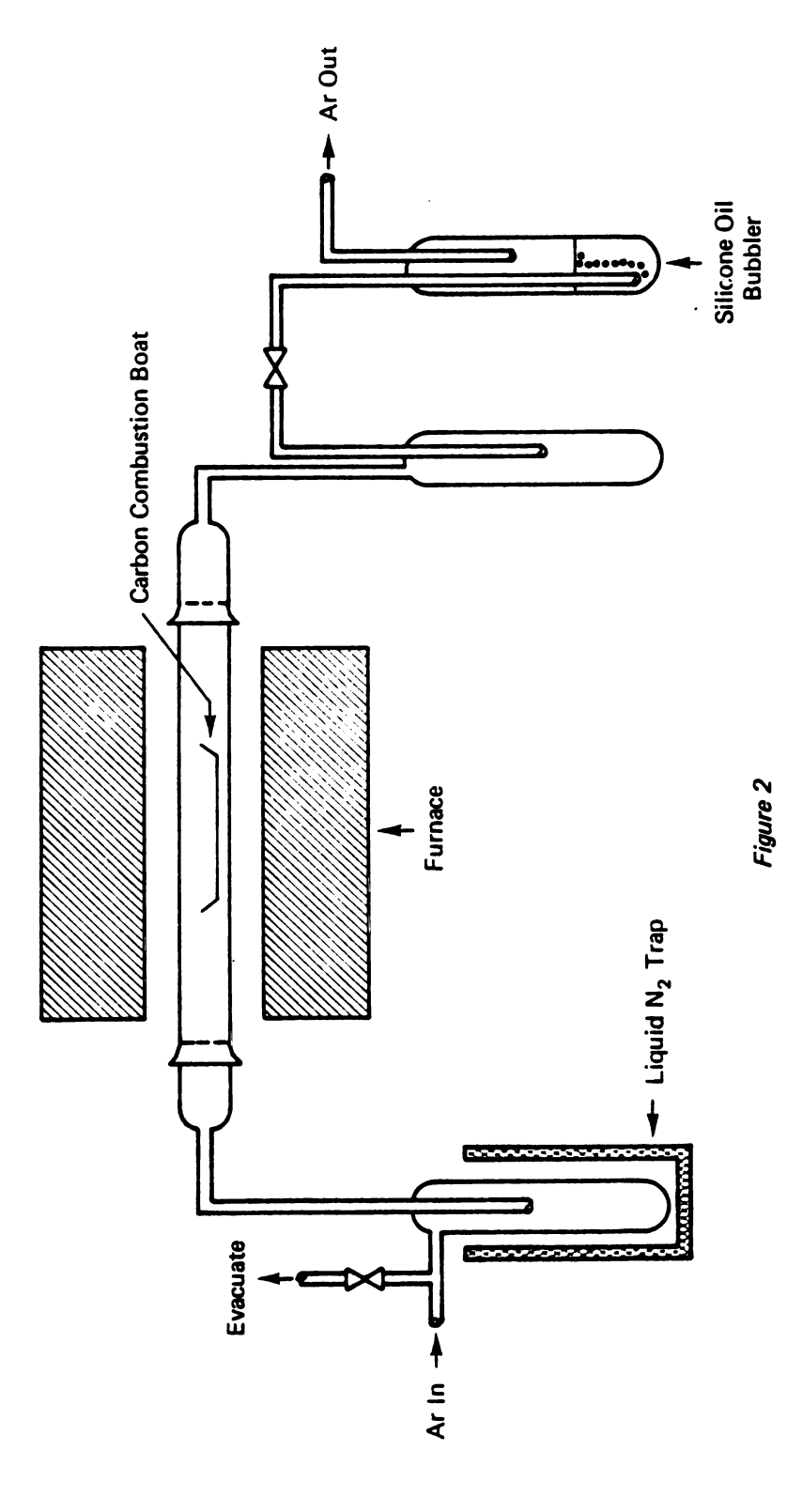
$$Sm_2O_3 + 6HBr(aq) - 2[SmBr_3 \cdot 6H_2O \cdot xNH_4Br]$$

$$NH_4Br$$
(excess)
(3a)

$$SmBr_3 \cdot 6H_2O \cdot xNH_4Br \xrightarrow{\Delta} SmBr_3 + 6H_2O(g) + xNH_4Br(g)$$
 (3b)

One gram of oxide was added to a 15 ml volume of 48% hydrobromic acid in a 150 ml beaker. The solution was heated on a hot plate and stirred until it became clear. Ammonium bromide (3.5 g) was added in a 13:1 molar ratio of ammonium bromide to metal ion. The mixture was heated to boiling until all the solids dissolved. The hot solution was transferred to a porcelain evaporating dish and heated to dryness. The resultant cream-colored powder was transferred to a vitreous carbon combustion boat and placed in the apparatus shown in Figure 2.

The sample was purged with dry argon for 30 minutes and heated to 200°C for 30 minutes. The temperature was increased in one hundred centigrade degree increments each hour up to 600°C. The sample was cooled to room temperature and heated to 500°C for one hour under a pressure of  $10^{-4}$  to  $10^{-5}$  torr. The sample was cooled, and transferred to an argon-filled Schlenk tube. The tube was evacuated and transferred to an argon-filled glove box where the sample was stored in a screw-capped glass vial.



Samarium Bromide Preparation Apparatus

#### Reduced and Mixed Valence Samarium Bromides

#### A. Sealed Containers

#### 1. Samarium Dibromide

Anhydrous samarium dibromide was prepared according to the following reaction:

$$Sm + 2SmBr_3 \longrightarrow 3SmBr_2 \tag{4}$$

A 0.165 g sample of -40 mesh samarium metal and a 0.840 g sample of anhydrous samarium tribromide were placed in an outgassed 8 x 120 mm quartz ampoule. The ampoule, after evacuation, was sealed with an oxygen-methane torch.

The sealed ampoule was placed in a horizontal tube furnace, heated to 800°C for a period of up to five hours, and annealed at 450°C for five hours. The ampoule was agitated periodically to insure homogeneity of the melt. The ampoule was cooled, transferred to a glove box, and the contents examined. The gray-black powder product was stored in a snap-capped glass vial in the glove box.

# 2. Sm<sub>6</sub>Br<sub>13</sub>

Mixed valence samarium bromide was prepared in a manner similar to that described for preparation of samarium dibromide. The reaction proceeded according to the following stoichiometry:

$$\frac{5}{3}$$
Sm +  $\frac{13}{3}$ SmBr<sub>3</sub> ----- Sm<sub>6</sub>Br<sub>13</sub> (5)

A 0.129 g sample of samarium metal was mixed and allowed to react with a 0.871 g sample of anhydrous samarium tribromide.

The resultant product was a fused black mass which exhibited a gray-black color when crushed.

# 3. Sm<sub>5</sub>YBr<sub>13</sub>

Samarium yttrium bromide was prepared in a manner similar to that described for preparation of samarium dibromide. Samarium metal, samarium tribromide and yttrium tribromide were reacted in evacuated, sealed quartz ampoules in the following stoichiometry:

$$\frac{5}{3}$$
Sm +  $\frac{10}{3}$ SmBr<sub>3</sub> + YBr<sub>3</sub> --- Sm<sub>5</sub>YBr<sub>13</sub> (6)

A 0.147 g sample of samarium metal was allowed to react with a mixture of 0.692 g samarium tribromide and 0.174 g yttrium tribromide.

The resultant product was a fused black mass that was gray-green to gray-black in color when ground.

# 4. Sm<sub>5</sub>HfBr<sub>13</sub>

An attempt was made to prepare samarium hafnium bromide according to the procedure outlined for the preparation of samarium dibromide. A sample of 0.153 g samarium metal, 0.593 g samarium tribromide and 0.253 g hafnium tetrabromide was allowed to react according to:

$$2Sm + 3SmBr_3 + HfBr_4 - Sm_5 HfBr_{13}$$
 (7)

The resultant fused black powder exhibited a gray-black color when crushed.

Since the quartz reaction vessels were potential samarium metal scavengers, slight stoichiometric excesses of metal were used routinely.

#### B. Open Containers

#### 1. Samarium Dibromide

Sealed quartz ampoules proved inadequate for the preparation of reduced and mixed valence samarium bromides due to formation of samarium oxide bromide:

$$2SmBr_3 + SiO_2 - 2SmOBr + SiBr_4$$
 (8)

The reaction is discussed in detail by Corbett. 51

Samarium dibromide, without oxide bromide contamination, was prepared in the following manner. A mixture of 0.165 g samarium metal and 0.840 g samarium tribromide was placed in a vitreous carbon combustion boat and a tantalum foil cover was tightly fitted over the boat. The boat was placed in a horizontal tube furnace, heated to 700°C for one hour under an argon pressure of one atmosphere, and annealed at 450°C for four hours. The product was cooled and transferred to a glove box. The resultant dibromide was a fused black mass which was gray-black in color when ground.

# 2. Sm<sub>6</sub>Br<sub>13</sub>

Mixed valence samarium bromide was prepared in vitreous carbon combustion boats by a procedure similar to that used for the preparation of samarium dibromide. A mixture of 0.128 g samarium metal and 0.869 g samarium tribromide was allowed to react to form a fused black mass of  $\rm Sm_6Br_{13}$  which was gray-black in color when crushed.

# 3. Sm<sub>5</sub>YBr<sub>13</sub>

Samarium yttrium bromide was prepared in vitreous carbon combustion boats according to the procedure used in the preparation of samarium dibromide. A mixture of 0.397 g samarium metal, 2.078 g samarium tribromide and 0.520 g yttrium tribromide was heated to 950°C for 15 minutes, 800°C for 1 hour, and annealed at 450°C for five hours. The resultant black fused product was gray-black in color when ground.

# 4. Sm<sub>5</sub>HfBr<sub>13</sub>

An attempt was made to prepare samarium hafnium bromide according to the procedure outlined for the preparation of samarium dibromide. A mixture of 0.154 g samarium metal, 0.596 g samarium tribromide and 0.253 g hafnium tetrabromide was allowed to react to form a fused black mass which was gray-black in color when ground.

#### Samarium Tribromide Hexahydrate

Hydrated samarium tribromide was prepared from the anhydrous tribromide. The anhydrous cream-colored tribromide was exposed to air at room temperature for 24 hours. The resultant white product was determined by X-ray powder diffraction to be SmBr<sub>3</sub>·6H<sub>2</sub>O.

#### Samarium Dibromide Monohydrate

Hydrated samarium dibromide was prepared in a manner similar to that described by Haschke. Black, anhydrous dibromide was exposed to air for a short period of time. The resultant monohydrate was red in color. Extended exposure of the monohydrate to atmospheric moisture resulted in the formation of the white, hydrated tribromide.

#### Yttrium Tribromide

Yttrium tribromide was prepared in a manner similar to that described for the preparation of anhydrous samarium tribromide. A 2 g sample of Y2O3 was dissolved in a 30 ml volume of 48% HBr. The solution was heated and a 7 g sample of NH4Br was added. The resultant yellow solution was transferred to a porcelain evaporating dish and heated to dryness. The dry, white powder was transferred to a vitreous carbon combustion boat and heated in the apparatus shown in Figure 2. The product was heated according to the schedule previously described for the preparation of anhydrous samarium tribromide.

#### Single Crystal Preparation

Single crystals of  $Sm_5YBr_{13}$  were prepared upon crystallization of a liquid melt upon slow cooling.

A sample of 0.147 g samarium metal, 0.695 g samarium tribromide and 0.174 g yttrium tribromide was sealed under vacuum in an outgassed quartz ampoule, heated to 1000°C for one hour and cooled to 675°C over a period of several days at a rate of 5°C/hour. The sample was then cooled to room temperature at a rate of 100°C/6 hours. The ampoule was transferred to a glove box, broken open and the gray product was lightly crushed. Examination of the product showed the existence of single crystals.

#### ELEMENTAL ANALYSES

#### Samarium Oxide Bromide

All bromide samples were analyzed for oxide bromide content. A 1 g sample of soluble bromide was dissolved in a 100 ml volume of water and the resultant mixture was acidified to pH 3-4 with 6 M nitric acid. The solution was stirred and filtered through a weighed, dry, glass-fritted weighing crucible. The crucible was heated to 300°C for four hours to dry the SmOBr.

The filtrate was saved and used for metal and bromide analyses.

#### Metal Analyses

### A. Conversion to Oxide

All unsubstituted samarium bromides were analyzed for samarium content by firing the bromide to the oxide, e.g.:

$$2SmBr_x + \frac{3}{2}O_2 - Sm_2O_3 + xBr_2$$
 (9)

A 0.5 g sample of samarium bromide was placed in a weighed, dry, procelain crucible. The crucible was fired to 900°C in a muffle furnace for six hours and cooled to room temperature. The crucible was reweighed and the amount of  $\rm Sm_2O_3$  formed was determined.

#### B. Atomic Absorption Spectroscopy

Transition-metal-substituted bromides and selected samarium bromides were analyzed for metal content by atomic absorption spectroscopy. Analyses were performed on a Perkin-Elmer instrument located in the 1602 Building Analytical Lab of the Michigan Division of The Dow Chemical Company, Midland, MI. All metals were analyzed using a reducing nitrous oxide-acetylene flame. Samarium was analyzed at 429.7 nm wavelength, yttrium at 410.2 nm and hafnium at 307.3 nm. Samarium and yttrium were partially ionized by a nitrous oxide-acetylene flame. Potassium nitrate solution was added at a concentration of 2000 ppm and 4000 ppm, respectively, to suppress ionization.

#### Bromide Analyses

Samarium bromide products were analyzed for bromide content by precipitation titration with silver nitrate and ferric ammonium sulfate or by atomic absorption spectroscopy.

#### A. Volhard Titration

The Volhard method is applicable for the determination of bromide in acid solution. The method is based on the insolubility of silver thiocyanate and uses ferric ion as the indicator to show when excess thiocyanate is present.

In the analysis a measured excess of standard silver solution is added to a bromide sample and the excess silver is titrated by a standard solution of thiocyanate:

$$Ag^+$$
 (excess) +  $Br^-$  AgBr +  $Ag^+$  (10)

$$Ag^{+} + SCN^{-} \longrightarrow AgSCN$$
 (11)

$$Fe^{3+} + 6SCN^{-} - Fe(SCN)_{6}^{3-}$$
 (red) (12)

A 0.1 g sample of soluble bromide was dissolved in a 50 ml volume of water. The solution was acidified to pH 3-4 with 1:1 nitric acid. A 25 ml volume of 0.1 M silver nitrate was added to the solution and the resultant mixture was titrated with 0.1 M potassium thiocyanate. Several drops of a saturated solution of ferric ammonium sulfate in 1:1 nitric acid was used as the indicator.

### B. Atomic Absorption Spectroscopy

All samarium bromide products were analyzed for bromide content by atomic absorption spectroscopy. Analyses were performed on a Varian Techtron instrument located in the Larkin Lab Building of the Central Research Inorganic Laboratory of The Dow Chemical Company, Midland, MI.

Bromide was analyzed by atomic absorption spectroscopy in a manner similar to that used in a Volhard titration; determination of excess silver added to a bromide solution. The excess silver was analyzed using an oxidizing airacetylene flame at 338.3 nm wavelength. The presence of other halides interferes with the analyses.

## X-RAY POWDER DIFFRACTION PATTERNS

Powder diffraction patterns of the various products were obtained using a Guinier focusing X-ray powder diffraction camera equipped with a fine focus copper X-ray tube ( $\lambda\alpha$  = 1.54050 Å). The camera had an effective radius of 80 mm. Platinum powder (a = 3.9237±0.0003 Å) was included in the samples prepared for powder diffraction analyses. The interplanar d-spacings of the powder patterns were based on this platinum standard.

Both a sample and a small amount of platinum powder were secured to an X-ray planchet (a steel disc with a 5 mm hole in the center) with amorphous transparent tape and covered with a piece of Parafilm M barrier film to minimize hydrolysis, which occurred upon prolonged exposure to air.

The planchet was placed in the X-ray holder, a magnet revolving at 50 rpm, with the back side of the tape against the magnet. The film cassette, which contained a 20 x 140 mm strip of Ilford Type G Industrial X-ray film encased in two sheets of black paper to prevent light exposure, was placed on the pin point triangular support of the camera box. incident beam stop on the camera was opened, the camera box closed for safety purposes, and the shutter on the X-ray tube was opened for ten seconds to expose the film to the incident beam. The beam stop was closed and the camera box was evacuated with a mechanical pump. The films were exposed to X-rays for six to twelve hours (35 kv at 20 ma, Picker Nuclear X-Ray Generator). Two noncoincident images were recorded on the film due to the sharp lines obtained and the angle of intersection of the diffracted beam with the film. Since an image was recorded on both sides of the film, one layer of film emulsion had to be removed. was accomplished with a small wire brush after the film had been densensitized by a fixing solution.

The diffraction lines on the film were measured precisely, to the nearest 0.001 inch, using a vernier-type film reader.  $\sin^2\theta$  and d-spacing values were calculated from observed data. Powder diffraction patterns were also calculated by a modification of the program, ANIFAC, prepared by Larson et al. <sup>52</sup> All cell parameters for the compound  $\cos^2\theta$  were calculated from the powder diffraction pattern by least squares regression analysis (Program Guinier). <sup>53</sup>

CHAPTER IV
RESULTS

#### ELEMENTAL ANALYSES

All prepared phases were analyzed for metal and bromide content. Corrections were made for SmoBr formation. Sample contamination by the oxide bromide was generally less than one percent by weight. The analytical results of several samarium bromide phases are outlined in Table III.

Prepared samples of the phase  $\mathrm{Sm_5HfBr_{13}}$  showed an absence of hafnium metal when analyzed by atomic absorption spectroscopy.

### X-RAY POWDER DIFFRACTION ANALYSES

Some assumptions were made in the X-ray powder diffraction analyses of several samarium bromide phases. positional parameters used in the ANIFAC determination of an SmBr, powder pattern were those obtained for a similar compound, SrBr<sub>2</sub>. 54 The powder pattern of Sm<sub>5</sub>Br<sub>11</sub> was calculated from the positional parameters obtained for  $Dy_5Cl_{11}$ . The thermal parameters of  $\mathrm{Dy_5Cl}_{11}$  were modified for  $\mathrm{Sm_5Br}_{11}$ due to density differences of the atoms. The powder patterns of Sm<sub>6</sub>Br<sub>13</sub> and Sm<sub>5</sub>YBr<sub>13</sub> were calculated with the positional parameters obtained for Yb5ErCl. 5 The positional parameters of  $Sm_6Br_{13}$  and  $Sm_5YBr_{13}$  were corrected from those of Yb<sub>5</sub>ErCl<sub>13</sub> by x-1/4; y-1/4; and z. Isotropic thermal parameters were used for the powder pattern calculations since the program ANIFAC would not evaluate anisotropic thermal parameters. The positional and thermal parameters used in the X-ray powder diffraction analyses of various

Analytical Results of Several Samarium Bromide Phases TABLE III:

	ပိ	Calculated			Actual*	
Phase	& Sm	8Y	&Br	&Sm	8.Y	8Br
${ m SmBr}_2$	49.47		51.53	48.75±0.05	!	51.20±0.14
$\mathrm{Sm}_{6}\mathrm{Br}_{13}$	46.48		53.52	46.62±0.08	-	53.68±0.10
$\mathrm{Sm}_{5}\mathrm{YBr}_{13}$	40.00	4.73	55.27	30.89±0.20	4.79±0.03	55.94±0.12
SmBr <sub>3</sub>	38.54		61.46	38.67±0.04	-	61.46±0.15

\*All results have been corrected for SmOBr contamination.

samarium bromide phases are listed in Appendices A, B and C.

Samarium yttrium bromide was indexed in space group C2/c for all X-ray powder diffraction intensity and lattice parameter calculations. The properties of space group C2/c are listed in Table IV. A representation of the symmetry of this space group is illustrated in Figure 3.

The X-ray powder diffraction patterns of all prepared compounds are outlined in Appendices D-M.

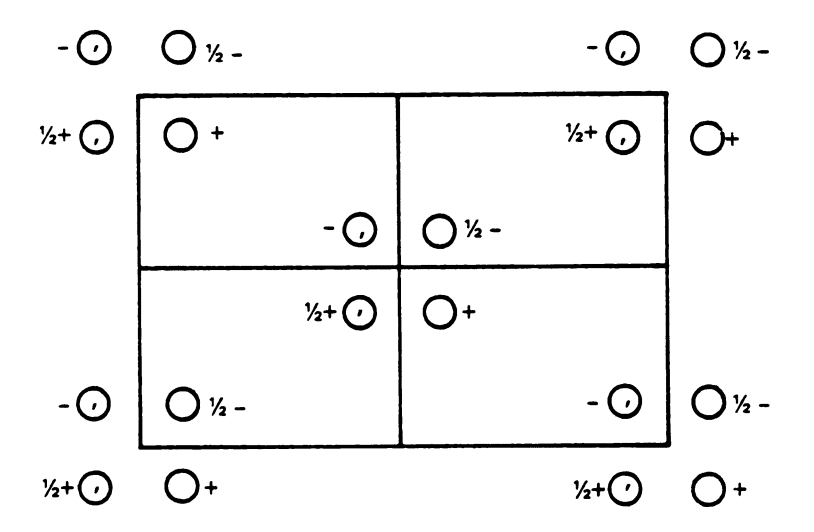
### CALCULATION OF LATTICE PARAMETERS

The lattice parameters of the compound,  $\mathrm{Sm_5YBr_{13}}$ , were refined by a least squares regression analysis. The crystal was of a monoclinic symmetry with a c-centered lattice. The refinement was based on the indexed reflections of the X-ray powder diffraction patterns. For the final calculation 58 reflections were used. The refined constants obtained were then used to calculate  $\sin^2\theta$  values. The result of the least squares refinement of the  $\mathrm{Sm_5YBr_{13}}$  lattice parameters is detailed in Appendix N.

The data obtained for  $\rm Sm_5YBr_{13}$  are listed in Table V. As previously mentioned, the lattice parameters of  $\rm Sm_6Br_{13}$  calculated by Bärnighausen<sup>3</sup> are likewise based on powder diffraction photographs. A comparison of the lattice parameters of  $\rm Sm_6Br_{13}$  is shown in Table VI. All parameters are based on the assignment of the compounds to space group C2/c.

TABLE IV: Properties of Space Group C2/c<sup>55</sup>

	······································	
Positions	Point Symmetry	Coordinates of Equivalent Positions
8 <b>f</b>	1	$(0,0,0; \frac{1}{2},\frac{1}{2},0) + x,y,z; \overline{x},\overline{y},\overline{z}; x,y,\frac{1}{2} - z;$
<b>4</b> e	2	$0, y, \frac{1}{4};  0, \overline{y}, \frac{3}{4}$
4d	Ī	$\frac{1}{4}, \frac{1}{4}, \frac{1}{2};  \frac{3}{4}, \frac{1}{4}, 0$
4c	· <u>1</u>	$\frac{1}{4}, \frac{1}{4}, 0; \frac{3}{4}, \frac{1}{4}, \frac{1}{2}$
4b	I	$0,\frac{1}{2},0; 0,\frac{1}{2},\frac{1}{2}$
4a	ī	$0,0,0; 0,0,\frac{1}{2}$



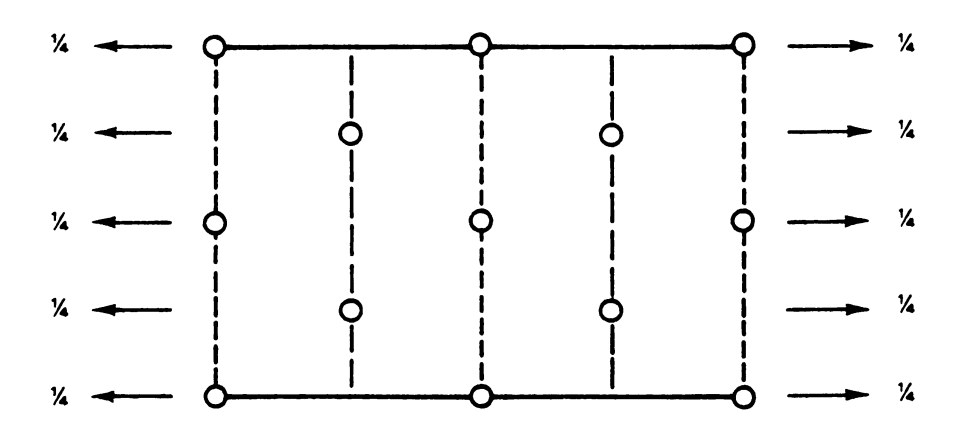


Figure 3

Representation of Space Group C2/c<sup>55</sup>

TABLE V: Data on Sm<sub>5</sub>YBr<sub>13</sub>

Space Group	C2/c
Unique axis	<u>b</u>
<u>a</u> (Å) *	44.31±0.05
<u>b</u> (Å)	7.139±0.008
<u>c</u> (Å)	6.651±0.008
<u>β</u> (°)	98.45±0.007
$\underline{\mathbf{v}}$ ( $\mathbf{\mathring{A}}^3$ )	2394
<u>z</u>	4
Formula Weight	1897.5
D <sub>calc</sub> (g/cm <sup>3</sup> )	5.21±0.03
t (°C)	23±3
λ (Å)	1.54050
General positions	$(\underline{x},\underline{y},\underline{z})$
(±)	$(\underline{x}, \frac{1}{2} - \underline{y}, \underline{z})$
	$(\frac{1}{2} + \underline{x}, \frac{1}{2} + \underline{y}, \underline{z})$
	$(\frac{1}{2} + \underline{x}, -\underline{y}, \frac{1}{2} + \underline{z})$
	Glide at $y = 0.25$ Glide at $z = 0.25$

<sup>\*</sup>Least squares fit.

TABLE VI: Comparison of Lattice Parameters\* of  $\mathrm{Sm_6^{Br}_{13}}$  and  $\mathrm{Sm_5^{YBr}_{13}}$ 

Parameter	Sm <sub>6</sub> Br <sub>13</sub> <sup>43</sup>	Sm <sub>5</sub> YBr <sub>13</sub>
a (Å)	43.97±0.08	44.31±0.05
<u>b</u> (Å)	7.139±0.002	7.139±0.008
<u>c</u> (Å)	7.649±0.002	7.651±0.008
β <b>(°)</b>	98.58±0.07	98.45±0.07
D <sub>calc</sub> (g/cm <sup>-3</sup> )	5.342	5.21±0.03
<u>v</u> (ų)	2401	2394

<sup>\*</sup>Space group C2/c

# SINGLE CRYSTAL PREPARATION

A mixture of SmBr<sub>3</sub>, Sm and YBr<sub>3</sub> was melted in a sealed, evacuated, quartz vessel and slowly cooled. The resultant product was crushed and examined visually under a microscope. The product included gray polycrystalline material and rectangular-prismatic crystals.

CHAPTER V

DISCUSSION

#### DISCUSSION

Unusual intermediate valence rare earth halides are well known. One such system that has been recently characterized is the SmBr, system. 4 Reported compositions include  $Sm_5Br_{11}$ ,  $Sm_{11}Br_{24}$  and  $Sm_6Br_{13}$ . Two of the compounds are defined by a well-studied homologous series,  $M_n X_{2n+1}$ , of rare earth halides. All of these compounds can also be described as members of the series  $M_n X_{2n+2}$  where n = 10, 11 and 12, respectively. 56 A major problem in studying mixed valence rare earth halides has been the inability to produce single crystals. Consequently, the lattice parameters of these compounds have been solved from the X-ray powder diffraction photographs of polycrystalline samples. Single crystals of  $\mathrm{Dy}_5\mathrm{Cl}_{11}$  were produced but they could not be obtained in the YbCl, or SmBr, systems. Single crystals of an intermediate valence ytterbium chloride were obtained as a mixed-metal phase. The resultant compound, Yb5ErCl13, was characterized by single crystal techniques and shown to be isostructural with the desired ytterbium phase. It is possible that substitution of another metal into the SmBr<sub>x</sub> lattice could also result in single crystal formation.

The close similarity between the ytterbium chloride, dysprosium chloride and samarium bromide systems can be understood by a simple radius-ratio argument. A comparison of the ionic radii of Cl/Yb and Br/Sm indicates a ratio of 1.84 and 1.80, <sup>57</sup> respectively, when the trivalent ions, with coordination number eight, are used for the rare earths.

The use of divalent rare earth radii should result in comparably identical ratios. The Cl/Dy ratio of 1.75 is similar to the Br/Sm value. Similarities among ratios can be expected elsewhere in the rare earth series, particularly among the bromide and iodide systems.

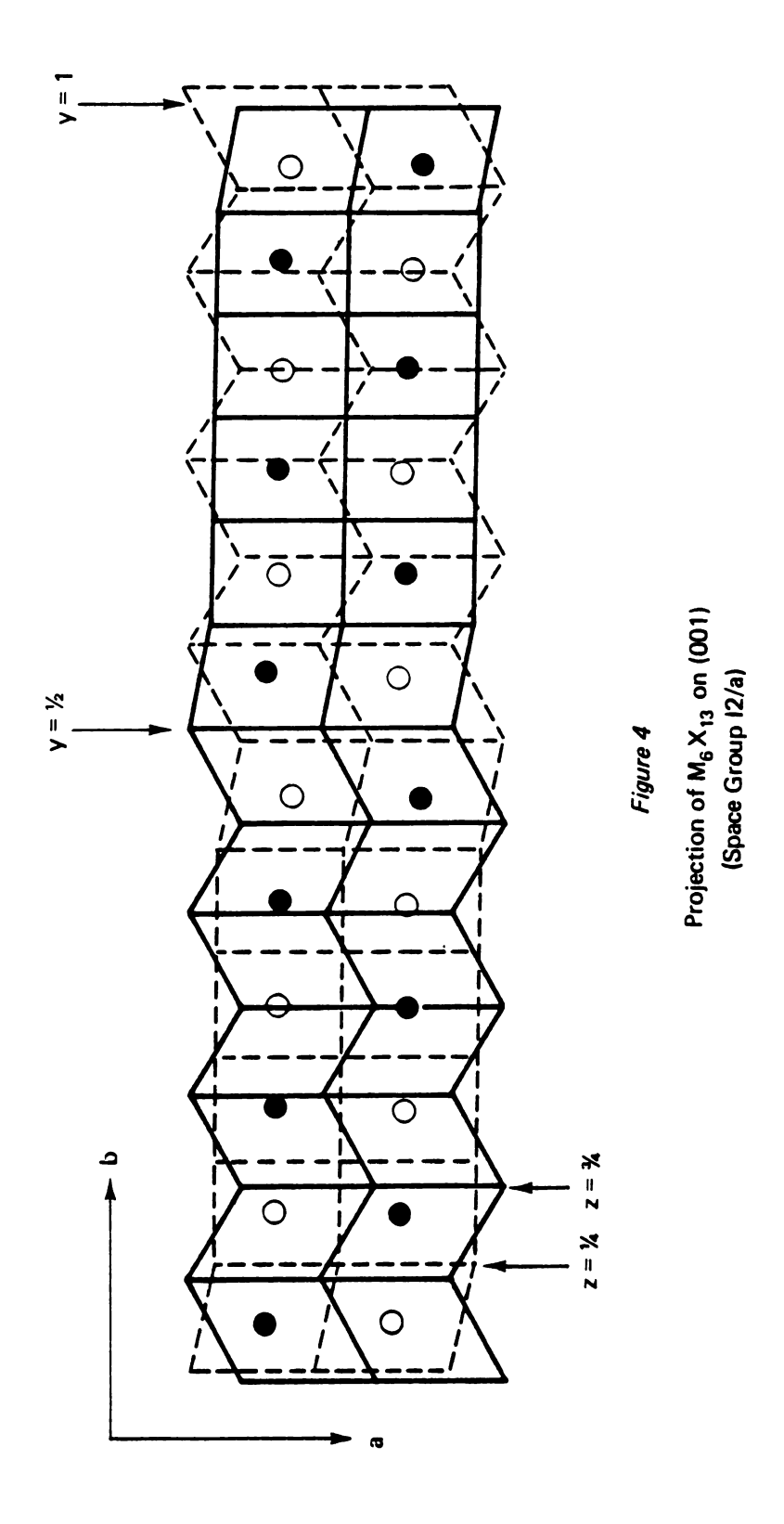
Mixed-metal rare earth halides have only been reported in isolated cases. As previously mentioned, such systems have resulted in excellent single crystal formation. Looking at the  ${\rm SmBr}_{\mathbf{x}}$  system several metals could be substituted into the crystal lattice. One such metal is yttrium. Trivalent yttrium, with an coordination number of eight has an crystal radius of 1.02 A. The resultant Br/Y ratio is The samarium-yttrium-bromide system is unique in that no transition metal has yet been substituted into the structure of a mixed valence rare earth halide. The compound  $Sr_ADyCl_{11}$  has been reported<sup>3</sup> but the substituted metal, strontium, is not a d-block metal and the rare earth, dysprosium, is not in a reduced valence state. The most interesting feature of yttrium, and some other transition metals, however, is their significantly lower electron density than the lanthanide metals. Incorporation of yttrium into the samarium bromide lattice should allow detection by X-ray analysis, of an ordered structure, if one exists. Presently, distinction between the  ${\rm M}^{2+}$  and  ${\rm M}^{3+}$  sites in the lattice cannot be made.

Another possible metal substitute is hafnium. Hafnium usually exists in the tetravalent state with an effective

radius of 0.83 Å. Trivalent hafnium has been reported, as  ${\rm HfI_3.}^{58}$  The radius of trivalent hafnium is expected to be larger than 0.83 Å and may yield a Br/Hf ratio similar to that seen for samarium and yttrium. The use of a bromide system may also help to stabilize hafnium in the trivalent state.

The proposed compounds,  $\rm Sm_5YBr_{13}$  and  $\rm Sm_5HfBr_{13}$ , should exhibit structures similar to those reported for  $\rm Dy_5Cl_{11}$ ,  $\rm Sm_6Br_{13}$  and  $\rm Yb_5ErCl_{13}$ . These compounds apparently belong to a class of vernier-type structures. This structure type has also been isolated in the compounds  $\rm Y_7O_6F_9$ ,  $\rm ^{32}Nb_2Zr_6O_{17}$  and  $\rm Zr_{108}N_{98}F_{138}$ ,  $\rm ^{34}$  and is discussed in detail by Hyde et al.  $\rm ^{31}$ 

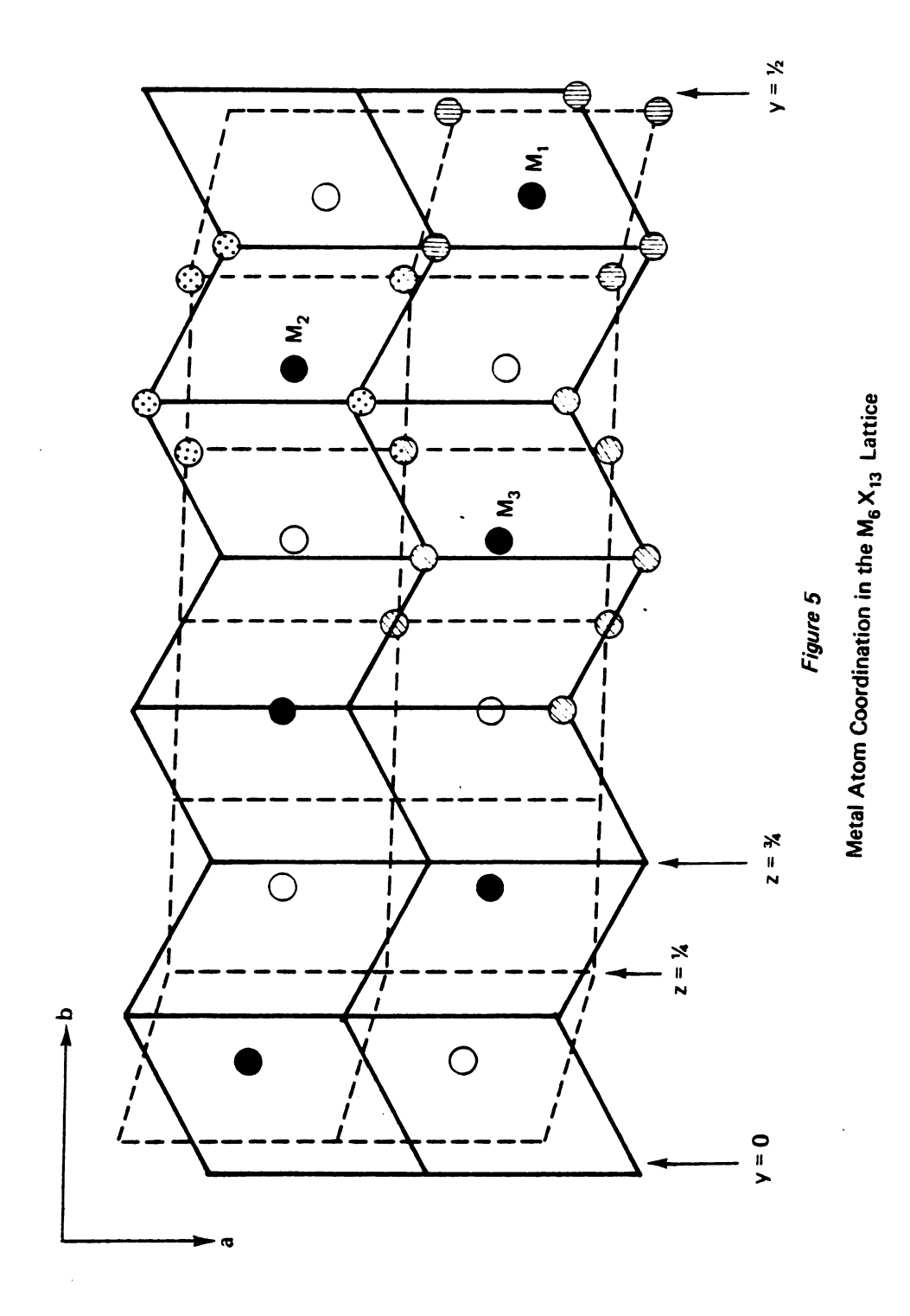
The vernier structures are of monoclinic symmetry. The structures are fluorite-type lattices. Compared to the fluorite structure, however, vernier unit cells contain additional anions, and the space required to accommodate these extra anions is obtained by transforming one half of the cubic anion packing into a hexagonal closest packing. Superimposition of these two anion layers leads to a vernier-type structure. For discussion purposes it is easier to visualize the structure in space group I2/a. A projection of the  $M_6X_{13}$  structure on (001) in such an orientation is shown in Figure 4. In this projection the metal atom arrangement in a fluorite lattice can be seen. The anion arrangement consists of two layers of atoms at z = 1/4 and z = 3/4. The lower layer is rectangular between y = 0 and



y=1/2, and the upper is a triangular net; the arrangement is reversed between y=1/2 and y=1. This arrangement allows for the space needed to accommodate the two extra anion rows. The open and filled circles indicate the position of the metal atoms at z=0 and z=1/2, respectively.

The anion coordination around the metal atoms is illustrated in Figure 5. One half of the unit cell is shown. The coordination around  $\mathrm{M}_1$  can be regarded as a capped octahedron. The  $\mathrm{M}_2$  site coordination may be regarded as a trigonal base-tetragonal base. A bicapped trigonal-prismatic coordination is observed surrounding  $\mathrm{M}_3$ . The structures of  $\mathrm{Sm}_5\mathrm{YBr}_{13}$  and  $\mathrm{Sm}_5\mathrm{HfBr}_{13}$  are expected to be similar to that of the detailed  $\mathrm{M}_6\mathrm{X}_{13}$  structure. Single crystal analyses of the two compounds may result in identification of the positions occupied by divalent and trivalent metal atoms.

The compound  $\rm Sm_5YBr_{13}$  can be prepared from a homogenous melt of samarium metal, samarium tribromide and yttrium tribromide. The reaction can be carried out in quartz reaction vessels but a high degree of product contamination by oxide bromide occurs. Quartz is also a samarium metal scavenger. A more suitable and practical reactor material is vitreous carbon. Haschke used carbon to prepare the mixed valence samarium bromide phases. A modification of his procedure proved effective in the preparation of  $\rm Sm_5YBr_{13}$ . The  $\rm SmBr_x$  preparation involved a reaction at 700-800°C under high vacuum (<10<sup>-4</sup> torr). This preparation



resulted in large losses of the tribromide through sublimation. Tribromide loss was minimized by heating the samarium-yttrium-bromide system under a one atmosphere pressure of dried argon.

The procedure used in the preparation of  $\mathrm{Sm}_5\mathrm{YBr}_{13}$  was not effective in the preparation of  $\mathrm{Sm}_5\mathrm{HfBr}_{13}$ . Hafnium tetrabromide sublimes at 420°C (one atmosphere pressure). Open containers of vitreous carbon proved unsuitable for preparation of this phase. The samarium hafnium bromide, likewise, could not be prepared in sealed quartz reactors. The unsuccessful attempts to produce  $\mathrm{Sm}_5\mathrm{HfBr}_{13}$  may be attributed to the inability to reduce hafnium to the trivalent state. The use of hafnium metal to form  $\mathrm{HfBr}_3$ , with the subsequent reaction with samarium, may lead to formation of  $\mathrm{Sm}_5\mathrm{HfBr}_{13}$ . Samarium in the lattice exists in the divalent state and could be produced separately (according to equation (4)) or in situ.

$$\frac{1}{4}\text{Hf} + \frac{3}{4}\text{HfBr}_4 + 5\text{SmBr}_2 \longrightarrow \text{Sm}_5\text{HfBr}_{13}$$
 (13)

$$\frac{1}{4} \text{Hf} + \frac{3}{4} \text{HfBr}_4 + \frac{5}{3} \text{Sm} + \frac{10}{3} \text{SmBr}_3 \longrightarrow \text{Sm}_5 \text{HfBr}_{13}$$
 (14)

The compound  $\rm Sm_5^{YBr}_{13}$  can be indexed in either the C2/c or I2/a space group. Lattice parameters calculated by least squares linear regression indicate  $\rm Sm_5^{YBr}_{13}$  is isostructural with  $\rm Sm_6^{Br}_{13}$ . Examination of the parameters shows the respective unit cells to be almost identical in size. Since the radius of Y<sup>3+</sup> is smaller than Sm<sup>3+</sup> (1.02 Å

compared to 1.09 Å) lattice parameters for  $\rm Sm_5YBr_{13}$  would be expected to be slightly smaller than those of  $\rm Sm_6Br_{13}$ . This size difference could also account for a slight decrease in the  $\beta$  angle.

A secondary objective of this work was to determine the ability of isolating single crystals of transition-metal-substituted samarium bromides. The ability to obtain single crystals supports the assumption that transition metals can be substituted into a stable, vernier lattice. The limit of non-lanthanide metal substitution is left to speculation. The information obtained in the growth of Sm<sub>5</sub>YBr<sub>13</sub> single crystals could be extended and adapted to other intermediate valence rare earth halide phases.

CHAPTER VI

CONCLUSION

#### CONCLUSION

The purpose of this work was to investigate a mixed valence rare earth halide. The system chosen was the vernier-structured compound,  $\mathrm{Sm_6Br_{13}}$ . Since single crystals of this compound had not been isolated, one of our goals was to produce a substituted samarium bromide that could be prepared in the form of single crystals. Work in the ytterbium chloride system<sup>5</sup> yielded single crystals after some substitution was made of another metal, with an ionic radius similar to ytterbium, into the crystal lattice.

On the basis of the ionic radius of  $\rm Sm^{3+}$ ,  $\rm r=1.09~\mathring{A}$ , two metals were chosen as possible candidates;  $\rm Y^{3+}$  where  $\rm r=1.02~\mathring{A}$  and hafnium. Hafnium normally exists in the tetravalent state,  $\rm r=0.83~\mathring{A}$ , but the existence of trivalent hafnium has been reported. Trivalent hafnium should have an  $\rm r>0.83~\mathring{A}$  and may approximate the radius of  $\rm Sm^{3+}$ . It was felt that the bromide ion in the system and the lattice energy might stabilize  $\rm Hf^{3+}$ . Transition metals, rather than rare earth metals, were chosen. The substitution of transition metals into the lattice of a rare earth halide may allow detection of an ordered structure if one exists. Also, the incorporation of transition metals into the vernier structure of rare earth halides has not been reported.

The unique compound,  $\mathrm{Sm}_5\mathrm{YBr}_{13}$  was prepared by reacting samarium metal with a mixture of samarium and yttrium tribromides at a temperature greater than the melting point

of the tribromides. The gray-black powder was analyzed by X-ray powder diffractometry. Least squares refinement of the powder pattern yielded unit cell lattice parameters comparable to those reported for  $\mathrm{Sm_6Br_{13}}$ . The vernier structure of  $\mathrm{Sm_5YBr_{13}}$  was also confirmed.

The attempts to produce single crystals of a transition-metal-substituted samarium bromide were successful. Growth of single crystals by the slow cooling of a homogeneous melt in quartz reactors was confirmed by microscopic observation. The crystals were of a rectangular-prismatic shape. Atomic parameter refinement of single crystals of  $Sm_5YBr_{13}$  should be an objective for future research.

All attempts to prepare  $\mathrm{Sm_5HfBr_{13}}$  from samarium metal, samarium tribromide and hafnium tetrabromide were unsuccessful. The inability to isolate this compound may be a result of the failure to reduce hafnium to the trivalent state. It might be possible to prepare the  $\mathrm{Sm_5HfBr_{13}}$  phase if hafnium metal is used to initiate reduction of tetravalent hafnium.

The ability to prepare and characterize the phase  $\mathrm{Sm}_5\mathrm{YBr}_{13}$  has led to an increase in the understanding of the structural aspects of mixed valence rare earth halides. The success of substituting another metal into the system to stabilize the lattice as well as the use of trivalent transition metals should lead to fruitful new areas of research.



#### REFERENCES

- 1. J. D. Corbett, <u>Preparative Inorganic Reactions</u>, <u>Vol. 3</u>, (W. L. Jolly, ed.), Interscience Publishers, New York, (1966).
- 2. J. D. Corbett, Rev. Chimie Min., 10, 239 (1973).
- 3. H. Bärnighausen, <u>Proc. Rare Earth Res. Conf.</u>, <u>12th</u>, <u>1</u>, 404 (1976).
- 4. J. M. Haschke, <u>Inorg. Chem.</u>, <u>15</u>, 298 (1976).
- 5. H. Lüke and H. A. Eick, <u>Proc. Rare Earth Res. Conf.</u>, 12th, <u>1</u>, 424 (1976).
- 6. C. Matignon, Compt. Rend., 134, 427 (1902).
- 7. M. D. Taylor, Chem. Rev., 62, 503 (1962).
- 8. F. Bourion, Compt. Rend., 148, 170 (1909).
- 9. Z. Darzens and F. Bourion, <u>Compt. Rend.</u>, <u>153</u>, 270 (1911).
- A. V. Davydov, S. S. Travnikov and B. F. Myasoedov,
   Zh. Anal. Khim., 26, (10), 1936 (1971).
- 11. P. Camboulive, Compt. Rend., 150, 175 (1910).
- 12. E. Chauvenet, Compt. Rend., 152, 87 (1911).
- 13. W. E. Domning and D. L. Schechter, U.S. Patent 3,153,570 (1964).
- 14. W. H. Baldwin, U. S. Patent 3,821,356 (1974).
- G. K. Borisov, S. G. Krasnova and R. I. Khranova, <u>Zh. Neorg. Khim.</u>, <u>16</u> (11), 2899 (1971).
- M. P. Taylor and C. P. Carter, J. <u>Inorg. Nucl. Chem.</u>, <u>24</u>, 387 (1962).
- 17. J. M. Haschke and H. A. Eick, J. <u>Inorg. Nucl. Chem.</u>, 32, 2153 (1970).

- 18. F. L. Carter and J. F. Murray, <u>Mat. Res. Bull.</u>, <u>7</u>, 519 (1972).
- O. G. Polyachenok and G. I. Novikov, <u>Zh. Neorg. Khim.</u>, <u>8</u> (7), 816 (1963).
- 20. R. E. Johnson and J. R. Mackenzie, <u>J. Inorg. Nucl.</u> Chem., <u>32</u>, 43 (1970).
- 21. C. W. DeKock and D. D. Radtke, J. <u>Inorg. Nucl. Chem.</u>, <u>32</u>, 3687 (1970).
- 22. D. E. Cox and F. K. Fong, <u>J. Cryst. Growth</u>, <u>20</u>, 233 (1973).
- 23. S. Mroczkowski, J. Cryst. Growth, 6, 147 (1970).
- 24. D. A. Lokken and J. D. Corbett, <u>Inorg. Chem.</u>, <u>12</u>, 556 (1973).
- 25. B. C. McCollum, M. J. Camp and J. D. Corbett, <u>Inorg.</u> Chem., <u>12</u>, 779 (1973).
- 26. K. R. Poeppelmeier and J. D. Corbett, <u>Inorg. Chem.</u>, <u>16</u>, 1107 (1977).
- 27. K. R. Poeppelmeier and J. D. Corbett, <u>Inorg. Chem.</u>, <u>16</u>, 294 (1977).
- 28. A. Simon, H. Mattausch and N. Holzer, Angew. Chem., <u>88</u>, 685 (1976).
- 29. R. L. Daake and J. D. Corbett, <u>Inorg. Chem.</u>, <u>16</u>, 2029 (1977).
- 30. A. W. Struss and J. D. Corbett, <u>Inorg. Chem.</u>, <u>9</u>, 1373 (1970).
- 31. B. G. Hyde, A. N. Bagshaw, S. Anderson and M. O'Keefe, Ann. Rev. Mat. Sci., 4, 43 (1974).
- 32. D. J. M. Bevan and A. W. Mann, Acta Cryst., B31, 1406 (1975).
- 33. J. Galy and R. S. Roth, <u>J. Solid State Chem.</u>, <u>7</u>, 277 (1973).
- 34. W. Jung and R. Juza, Z. Anorg. Allg. Chem., 399, 129 (1973).
- 35. J. D. Corbett, L. F. Druding, W. J. Burkhard and C. B. Lindahl, Discuss. Faraday Soc., 32, 79 (1961).

- 36. R. A. Sallach and J. D. Corbett, <u>Inorg. Chem.</u>, <u>2</u>, 457 (1963).
- 37. H. Bärnighausen, H. P. Beck and H. W. Grueninger, Proc. Rare Earth Res. Conf., 9th, 1, 74 (1971).
- 38. L. F. Druding and J. D. Corbett, <u>J. Am. Chem. Soc.</u>, <u>83</u>, 2462 (1961).
- 39. G. I. Novikov and O. G. Polyachenok, <u>Zh. Neorg. Khim.</u>, <u>8</u>, 1053 (1963).
- 40. L. F. Druding, J. D. Corbett and N. B. Ramsey, <u>Inorg.</u> Chem., <u>2</u>, 869 (1963).
- 41. J. J. Stezowski and H. A. Eick, <u>Inorg. Chem.</u>, <u>9</u>, 1102 (1970).
- 42. N. A. Fishel and H. A. Eick, <u>J. Inorg. Nucl. Chem.</u>, <u>33</u>, 1201 (1971).
- 43. O. G. Polyachenok and G. I. Novikov, <u>Zh. Neorg. Khim.</u>, <u>8</u>, 2818 (1963).
- 44. V. Loechner, H. Bärnighausen and J. D. Corbett, <u>Inorg.</u> <u>Chem.</u>, <u>16</u>, 2134 (1977).
- 45. J. D. Corbett and B. C. McCollum, <u>Inorg. Chem.</u>,  $\underline{5}$ , 938 (1966).
- 46. P. E. Caro and J. D. Corbett, <u>J. Less-Common Met.</u>, <u>18</u>, 1 (1969).
- 47. R. W. G. Wyckoff, <u>Crystal Structures</u>, <u>Vol. 2</u>, <u>2nd ed.</u>, <u>Interscience Publishers</u>, <u>New York</u> (1963).
- 48. M. Marenzio, H. A. Plettinger and W. H. Zachariasen, Acta Cryst., 14, 234 (1961).
- 49. D. Brown, S. Fletcher and D. G. Holah, <u>J. Chem. Soc.</u>, <u>A</u>, 1889 (1968).
- 50. A. V. Hariharan, Ph.D. Thesis, Michigan State University, East Lansing, MI. (1971).
- 51. J. D. Corbett, <u>Inorg. Nucl. Chem. Letters</u>, <u>8</u>, 337 (1972).
- 52. A. C. Larson, R. B. Roof and D. T. Cromer, "Anisotropic Structure Factor Calculation and Powder Pattern Generation," Los Alamos Laboratory Publication LA-3335 (1965).

- 53. O. Lindquist and F. Wengelin, <u>Ark. Kemi.</u>, <u>28</u>, 179 (1967).
- 54. J. G. Smeggil and H. A. Eick, <u>Inorg. Chem.</u>, <u>10</u>, 1458, (1971).
- 55. N. F. M Henry and K. Lonsdale, Ed., <u>International</u>

  <u>Tables for X-ray Crystallography</u>, <u>Vol. 1</u>, <u>International</u>

  <u>Union of Crystallography</u>, <u>Kynoch Press</u>, <u>Birmingham</u>,

  (1952).
- 56. H. Bärnighausen and J. M. Haschke, to be published in Inorg. Chem., (1978).
- 57. R. D. Shannon, Acta Cryst., A, 751 (1976).
- 58. A. W. Struss and J. D. Corbett, <u>Inorg. Chem.</u>, <u>8</u>, 277 (1969).



Appendix A: The Positional and Thermal Parameters of SmBr<sub>2</sub>\*

Atom	ж	У	Z	B(A <sup>2</sup> )**
- (2)		0.5054	0.0476	2.15
Sm(1)	0.1045	0.5856	0.2476	2.15
Sm (2)	0.2500	0.2500	0.8483	1.25
Br(1)	0.1531	0.4590	0.6258	3.33
Br(2)	0.3388	0.4572	0.0963	2.43
Br(3)	0.2500	0.7500	0.0000	2.90
Br(4)	0.2500	0.7500	0.5000	2.44

<sup>\*</sup>Based upon  $\operatorname{SrBr}_2^{54}$ 

<sup>\*\*</sup>Estimated

Appendix B: The Positional and Thermal Parameters of  $Sm_5Br_{11}^*$ 

Atom	х	У	z	B(A <sup>2</sup> )**
Sm(1)	0.3343	0.44475	0.0232	1.43
Sm (2)	0.7404	0.34558	0.0138	1.38
Sm (3)	0.3285	0.25000	0.0156	1.31
Sm (4)	0.8351	0.44492	0.4711	1.31
Sm (5)	0.2439	0.34504	0.4795	1.42
Sm (6)	0.8352	0.25000	0.4797	1.07
Br(1)	0.6100	0.49107	0.2317	2.05
Br(2)	0.6577	0.41724	0.8107	2.21
Br(3)	0.5353	0.39504	0.3037	2.05
Br (4)	0.3733	0.33080	0.8728	1.94
Br(5)	0.5453	0.29628	0.3144	1.52
Br(6)	0.6887	0.25000	0.8596	3.20
Br(7)	0.1035	0.49212	0.2732	2.52
Br(8)	0.1499	0.41714	0.6738	1.89
Br(9)	0.0247	0.39582	0.1938	1.69
Br(10)	0.1164	0.32758	0.6312	2.37
Br (11)	0.0305	0.29662	0.1885	1.40
Br(12)	0.1979	0.25000	0.6093	2.46

<sup>\*</sup>Based upon Dy<sub>5</sub>Cl<sub>11</sub><sup>3</sup>

<sup>\*\*</sup>Estimated

Appendix C: The Positional and Thermal Parameters of  $Sm_6Br_{13}$  and  $Sm_5YBr_{13}$ \*

Atom**	х	У	Z	B(Å <sup>2</sup> )***
Sm(1)	0.4542	0.2747	0.8750	1.32
Sm (2)	0.3705	0.2718	0.4010	1.32
Sm(3)	0.2900	0.2684	0.7407	1.32
Br(1)	0.4925	0.4816	0.6367	2.11
Br(2)	0.4307	0.0696	0.5347	2.11
Br(3)	0.4122	0.4452	0.1516	2.11
Br(4)	0.3555	0.1059	0.7419	2.11
Br (5)	0.3299	0.4400	0.0693	2.11
Br(6)	0.2838	0.1193	0.3678	2.11
Br(7)	0.2500	0.4413	0.0001	2.11

<sup>\*</sup>Based upon  $Yb_5ErCl_{13}^5$ \*\*Corrected Positional Parameters are  $x - \frac{1}{4}$ ;  $y - \frac{1}{2}$ ;  $z - \frac{1}{4}$ .

<sup>\*\*\*</sup>Estimated

Appendix D: X-Ray Powder Diffraction Pattern of Tetragonal SmBr<sub>2</sub>

h	k	Ł	d-value Calculated	(A) Observed	Observed Intensity
1	1	0	8.1940	8.1011	w
0	0	2	3.5500	3.5627	m
0	1	2	3.3943	3.3936	υω
1	1	2	3.2574	3.2170	υω
1	2	2	2.9287	2.9339	ω
0	3	2	2.6138	2.6111	w
2	4	0	2.5912	2.5843	w
1	3	2	2.5497	2.5477	w
2	4	1	2.4341	2.4314	vw
1	4	2	2.2035	2.2149	m
1	2	3	2.1528	2.1527	vw
2	5	1	2.0593	2.0584	w
4	5	2	1.6123	1.6138	m

Appendix E: X-Ray Powder Diffraction Pattern of Orthorhombic SmBr<sub>2</sub>·H<sub>2</sub>O

				alue (A)	Observed
h 	k —	<u> </u>	Calculated	Observed	Intensity
2	0	0	4.5890	4.5821	ω
1	2	1	3.2239	3.2289	ω
2	0	1	3.1436	3.1376	υω
3	0	0	3.0593	3.0771	w
2	1	1	3.0310	3.0452	w
3	1	0	2.9552	2.9533	ω
0	3	1	2.8556	2.8785	υω
2	2	1	2.7542	2.7826	ω
3	2	0	2.6970	2.6703	ω
3	0	1	2.4957	2.5097	m
3	1	1	2.4382	2.4493	υω
0	0	2	2.1575	2.1573	υω
0	1	2	2.1200	2.1208	υω

Appendix F: X-Ray Powder Diffraction Pattern of Orthorhombic SmBr<sub>3</sub>

		d-value	(A)	Observed
h k	l	Calculated	Observed	Intensity
0 1	1	7.4112	7.300	ω
	0	6.3530	6.3905	m
0 2	1	5.2136	5.2478	w
0 0	2	4.5620	4.5606	m
1 1	1	3.5485	3.5416	ω
1 0	2	3.0253	3.0148	ω
1 1	2	2.9431	2.9454	ω
1 3	0	2.9241	2.9264	m
1 3	1	2.7846	2.7876	\$
0 2	3	2.7432	2.7434	m
1 2	2	2.7314	2.7240	m
0 3	3	2.4704	2.4717	w
1 1	. 3	2.3870	2.3857	\$
1 2	3	2.2498	2.2510	\$
1 3	3	2.1079	2.1064	w
2 0	0	2.0210	2.0219	m
2 1	. 0	1.9959	2.0078	m
2 1	. 1	1.9498	1.9487	m

Appendix G: X-Ray Powder Diffraction Pattern of Monoclinic SmBr<sub>3</sub>·6H<sub>2</sub>O

	d-val	lue (A)	Observed
h k l	Calculated	Observed	Intensity
0 0 1	8.1422	8.0792	w
0 1 0	6.7620	6.8446	m
T 0 1	6.6184	6.6110	8
1 0 1	6.1324	6.2048	<b>&amp;</b>
1 1 0	5.6034	5.6750	m
0 0 1	5.2020	5.2576	m
2 0 0	5.0053	5.0398	m
<u>T</u> 1 1	4.6930	4.7269	۵
1 1 1	4.5426	4.5676	\$
0 0 2	4.0711	4.1037	8
1 0 2	3.6918	3.7042	8
2 1 1	3.5372	3.5596	8
0 1 2	3.4878	3.5064	w
0 2 0	3.3810	3.3885	w
2 0 2	3.2592	3.2762	vw
1 2 0	3.2032	3.2125	m
3 0 1	3.1574	3.1734	υω
0 2 1	3.1225	3.1314	m
3 0 1	3.0223	3.0302	m
<u>1</u> 2 1	3.0013	3.0046	m
1 2 1	2.9608	2.9723	m
<del>2</del> 1 2	2.9360	2.9477	m

Appendix G (Cont'd):

	d-val	ue (A)	Observed
h k l	Calculated	Observed	Intensity
3 1 1	2.8609	2.8697	vw
2 2 0	2.8017	2.8006	\$
3 1 1	2.7592	2.7696	ω
2 2 1	2.6781	2.6851	m
2 2 1	2.6213	2.6262	m
0 2 2	2.6010	2.6098	m
1 0 3	2.5792	2.5884	m
<u>1</u> 2 2	2.5421	2.5491	m
3 0 2	2.5054	2.5098	m
1 2 2	2.4934	2.4864	m
1 1 3	2.4099	2.4188	m
3 2 0	2.3750	2.3791	۵
4 0 1	2.3514	2.3571	m
3 2 1	2.3076	2.3111	۵
4 1 1	2.2911	2.2945	ω
4 1 1	2.2210	2.2237	ω
2 1 3	2.1995	2.2056	m
1 3 0	2.1989	2.1978	m
Ī 3 1	2.1302	2.1342	m
0 2 3	2.1165	2.1185	m
3 2 2	2.0922	2.0961	m
4 0 2	2.0751	2.0768	ω
2 3 0	2.0552	2.0562	υω

Appendix H: X-Ray Powder Diffraction Pattern of Tetragonal SmOBr

	d-valu	ie (A)	Observed
h k l 	Calculated	Observed	Intensity
0 0 1	7.9041	7.9475	m
0 0 2	3.9672	3.9556	υω
1 0 1	3.5312	3.5110	ω
1 1 0	2.7944	2.7976	m
1 1 2	2.2780	2.2488	νω
1 0 3	2.1934	2.2082	υω
2 0 0	1.9758	1.9720	w
2 0 1	1.9151	1.9028	ω
2 0 2	1.7677	1.7543	w
2 1 1	1.7230	1.7098	w
2 1 2	1.6146	1.6131	m
0 0 6	1.3172	1.3079	υω
1 0 6	1.2490	1.2405	m

Appendix I: X-Ray Powder Diffraction Pattern of Vernier  $Sm_5Br_{11}$ 

h	k	Ł	d-value Calculated	(A) Observed <sup>4</sup>	Observed Intensity
1	1	0	7.0536	7.028	·
1	1	ī	5.2281	5.235	w
5	1	1	4.2879	4.285	m
7	1	I	4.2270	4.269	m
2	0	2	3.8346	3.837	w
12	0	0	3.6670	3.722	w
1	1	2	3.3740	3.371	w
3	1	2	3.3639	3.357	w
2	2	ī	3.2278	3.225	w
6	2	0	3.2121	3.214	w
7	1	2	3.1339	3.101	m
4	2	1.	3.0487	3.058	m
11	1	1	3.0237	3.028	m
13	1	ī	2.9810	2.967	w
9	1	2	2.9522	2.957	w
6	2	1	2.8901	2.870	w
12	0	2	2.8597	2.861	w
10	0	2	2.6801	2.667	8
2	2	2	2.6141	2.615	m
0	0	2	2.6004	2.600	w
12	2	0	2.5591	2.615	8
2	2	2	2.5520	2.536	w

Appendix I (Cont'd):

h	k	Ł	d-value Calculated	(A) Observed	Observed Intensity
4	2	2	2.4742	2.469	m
12	0	2	2.4577	2.456	w
3	1	3	2.4070	2.408	m
1	1	3	2.3981	2.402	m
17	1	1	2.2275	2.242	m
5	3	1	2.1767	2.174	m
7	3	I	2.1687	2.168	m
16	0	2	2.0824	2.082	w
9	1	3	2.0318	2.020	w


Appendix J: X-Ray Powder Diffraction Pattern of Vernier Sm<sub>6</sub>Br<sub>13</sub>

			d-val	ue (A)	Observed
h'	k	Ł	Calculated	Observed	Intensity
3	1	0	6.4177	6.3715	w
1	1	ī	5.2183	5.2138	w
3	1	ī	5.0578	5.0005	vw
7	1	0	4.7149	4.6891	w
5	1	1	4.2848	4.3030	8
7	1	ī	4.2165	4.2428	· <b>m</b>
2	0	2	3.8233	3.7024	s
1	1	2	3.3662	3.3809	υω
8	0	2	3.3553	3.3509	w
2	2	ī	3.2232	3.1979	m
3	1	2	3.1704	3.1740	vw
4	2	1	3.0459	3.0681	υω
6	2	ī	3.0252	3.0290	m
11	1	1	3.0223	2.9999	w
13	1	ī	2.9743	2.9626	w
9	1	2	2.9428	2.9418	w
12	0	2	2.8497	2.8530	w
7	1	2	2.8029	2.7990	m
10	0	2	2.6785	2.6601	w
14	0	2	2.6126	2.6093	vw
2	2	2	2.6091	2.5932	vw
12	2	0	2.5564	2.5502	ω

Appendix J (Cont'd):

			d-value	(A)	Observed
<u>h</u>	k	L_	Calculated	Observed	Intensity
2	2	2	2.5489	2.5198	m
4	2	2	2.4712	2.4696	` <b>, m</b>
9	1	3	2.2654	2.2316	υω
12	2	2	2.2271	2.2210	υω
7	3	ī	2.1657	2.1669	υω
10	2	2	2.1424	2.1480	ω
7	3	1	2.1052	2.0926	w
16	0	2	2.0816	2.0776	vw
15	1	3	1.9865	2.0080	w
2	0	4	1.9086	1.9137	vw
10	4	ī	1.6345	1.6379	υω
19	3	2	1.5819	1.6039	υω

Appendix K: X-Ray Powder Diffraction Pattern of Monoclinic YBr3

d-value (A)		d-value (A)	
Observed	Intensity	Observed	Intensity
8.3924	νω	2.7970	\$
7.5313	m	2.7495	VW
7.1219	υω	2.7066	w
6.7456	υω	2.6085	w
6.4499	m	2.5596	υω
6.0259	\$	2.5301	υω
5.6154	m	2.4965	m
5.2240	υω	2.4770	m
5.0042	m	2.3521	ω
4.6738	νω	2.2331	ω
4.5990	m	2.2110	m
4.0415	ω	2.1774	w
3.6598	ω	2.1089	ω
3.5958	ω	2.0793	m
3.5064	m	2.0498	m
3.3295	m	2.0394	m
3.1945	m	1.9155	νω
3.1400	ω	1.8595	ω
3.1008	m	1.8250	υω
3.0403	ω	1.7889	υω
3.0054	m	1.7480	vw
2.9750	m	1.6590	vw

Appendix L: X-Ray Powder Diffraction Pattern of Vernier Sm<sub>5</sub>YBr<sub>13</sub>

			d-yalue	(Å)	Observed
h_	k —	l	Calculated	Observed	Intensity
5	1	0	5.5356	5.5970	νω
1	1	ī	5.2191	5.2038	υω
5	1	1	4.2826	4.2885	w
7	1	1	4.2114	4.2478	w
1	1	2	3.3671	3.3755	w
8	0	2	3.3525	3.3581	ω
2	2	Ι	3.2234	3.2217	ω
3	1	2	3.1709	3.1843	ω
7	1	2	3.1226	3.1164	ω
4	2	1	3.0456	3.0350	m
11	1	1	3.0176	3.0291	m
18	1	ī	2.9678	2.9702	ω
6	2	1	2.8868	2.8698	υω
7	1	2	2.8020	2.8199	۵
10	0	2	2.6763	2.6675	ω
14	0	2	2.6077	2.6308	w
2	2	2	2.6095	2.6044	vw
12	2	0	2.5529	2.5686	ω
4	2	2	2.4713	2.4650	т
12	0	2	2.4539	2.4687	m
8	2	2	2.4437	2.4378	w
3	1	3	2.4010	2.4008	w

Appendix L: (Cont'd):

				lue (A)	Observed
h	k	<u> </u>	Calculated	Observed	Intensity
3	3	1	2.2854	2.2455	w
13	1	2	2.2334	2.2347	w
12	2	2	2.2249	2.2319	w
20	0	0	2.1943	2.2021	w
7	3	ī	2.1650	2.1659	υω
16	0	2	2.0786	2.0779	ω
11	1	3	1.9281	1.9280	υω
15	3	0	1.8452	1.8470	υω
24	0	0	1.8262	1.8278	υω
13	1	4	1.7128	1.7174	υω
3	3	3	1.6992	1.6985	υω
26	0	0	1.6857	1.6857	υω
17	3	1	1.6677	1.6722	νω
10	4	1	1.6340	1.6371	νω
17	1	4	1.6030	1.6046	w
19	3	1	1.5835	1.5853	vw
15	3	3	1.5599	1.5607	vw
10	2	4	1.4985	1.4977	vw
22	0	4	1.4852	1.4780	vw
21	3	3	1.4038	1.4044	υw
22	2	4	1.3713	1.3750	υω

Appendix M: X-Ray Powder Diffraction
Pattern of Cubic HfBr<sub>4</sub>

h k l	d-value Calculated	(Å) Observed	Observed Intensity
1 1 1	6.2937	6.3427	w
2 0 0	5.4662	5.4789	ω
3 1 1	3.3022	3.2552	w
2 2 2	3.1500	3.0350	νω
3 2 1	2.9147	2.9231	w
4 0 0	2.7276	2.7380	vw
5 1 1	2.0991	2.1062	w
5 2 1	1.9933	1.9468	\$
5 2 2	1.9004	1.8997	w
6 0 0	1.8185	1.8281	w
8 1 1	1.3431	1.3769	m

Appendix N: Least Squares Refinement of  $${\rm Sm}_5{\rm YBr}_{13}$$  Lattice Parameters

	sin	2 <sub>θ</sub>		d-values	(A)
hkl	Observed	Calculated	Difference	Observed	
5 1 0	0.018939	0.019361	-0.000422	5.59697	5.53564
111	0.021909	0.021781	0.000128	5.20380	5.21907
5 1 1	0.032259	0.032348	-0.000089	4.28851	4.28260
7 1 1	0.032880	0.033451	-0.000571	4.24782	4.21141
1 1 2	0.052070	0.052331	-0.000261	3,37550	3.36707
8 0 2	0.052610	0.052788	-0.000178	3,35813	3.35246
3 1 2	0.052610	0.052699	-0.000089	3,35813	3.35529
2 2 1	0.057160	0.057101	0.000059	3.22170	3.22337
3 1 2	0.058510	0.059007	-0.000497	3.18432	3.17088
7 1 2	0.061090	0.060847	0.000243	3.11635	3.12257
4 2 1	0.064410	0.063962	0.000448	3.03497	3.04558
11 1 1	0.064659	0.065152	-0.000493	3.02913	3.01764
13 1 T	0.067250	0.067359	-0.000109	2.97020	2.96779
6 2 1	0.072039	0.071190	0.000849	2.86978	2.88684
7 1 2	0.074609	0.075567	-0.000958	2.81992	2.80198
10 0 2	0.083380	0.082833	0.000547	2.66748	2.67627
$14 \ 0 \ \overline{2}$	0.085719	0.087247	-0.001528	2.63083	2.60769

Appendix N: (Cont'd)

	sin	$^{2}_{ heta}$		d-values	o ues (A)
7 4 4	Observed		Difference	Observed	
2 2 2	0.087470	0.087125	0.000345	2.60437	2.60952
12 2 0	0.089920	0.091033	-0.001113	2.56864	2.55289
4 2 2	0.097640	0.097140	0.000500	2.46501	2.47134
12 0 2	0.097350	0.098526	-0.001176	2.46867	2.45390
8 2 2	0.099829	0.099347	0.000482	2.43783	2.44374
3 1 3	0.102930	0.102914	0.000016	2.40083	2.40101
3 3 <u>1</u>	0.117659	0.116318	0.001341	2.24553	2.25844
14 0 2	0.117659	0.116689	0.000970	2.24553	2.25485
13 1 2	0.118799	0.118938	-0.000139	2.23473	2.23343
12 2 2	0.119099	0.119849	-0.000750	2.23191	2.22492
17 1 1	0.119099	0.120193	-0.001094	2.23191	2.22173
20 0 0	0.122349	0.123540	-0.001191	2.20207	2.19143
19 1 T	0.122349	0.123504	-0.001155	2.20207	2.19175
731	0.126470	0.126569	-0.000099	2.16590	2.16505
16 0 2	0.137410	0.137323	0.000087	2.07789	2.07855
11 1 3	0.159600	0.159586	0.000014	1.92804	1.92812
15 3 0	0.173919	0.174249	-0.000330	1.84696	1.84521
13 3 1	0.173919	0.174146	-0.000227	1.84696	1.84576
3 1 4	0.173919	0.173846	0.000073	1.84696	1.84735

Appendix N: (Cont'd.)

	sin	$^{2}_{\theta}$		d-values	ues (A)
hkl	Observed	Calculated	Difference	Observed	Calculated
24 0 0	0.177579	0.177897	-0.000318	1.82783	1.82620
13 1 4	0.201150	0.202233	-0.001083	1.71740	1.71280
7 3 3	0.201150	0.202077	-0.000927	1.71740	1.71346
3 3 3	0.205659	0.205495	0.000164	1.09847	1.69915
26 0 0	0.208779	0.208782	-0.000003	1.68573	1.68572
17 3 1	0.212170	0.213311	-0.001141	1.67221	1.66773
10 4 1	0.221359	0.22222	-0.000863	1.63713	1.63395
10 2 4	0.221359	0.222150	-0.000791	1.63713	1.63421
14 2 3	0.221359	0.222401	-0.001042	1.63713	1.63329
17 1 4	0.230419	0.230883	-0.000464	1.60462	1.60301
12 4 0	0.230419	0.230710	-0.000291	1.60462	1.60361
19 3 1	0.236069	0.236600	-0.000531	1.58530	1.58352
15 3 3	0.243579	0.243817	-0.000238	1.56067	1.55991
10 2 4	0.264490	0.264209	0.000281	1.49771	1.49850
14 4 1	0.264490	0.264489	0.000001	1.49771	1.49771
22 0 4	0.271580	0.268954	0.002626	1.47803	1.48523
26 2 2	0.271580	0.269437	0.002143	1.47803	1.48389

Appendix N: (Cont'd.)

	sin	n 2 <sub>θ</sub>		d-valı	d-values (A)
१ ४ ५	Observed	Calculated	Difference	Observed	Calculated
21 3 3	0.300810	0.301065	-0.000255	1.40438	1.40379
734	0.300810	0.300348	0.000462	1.40438	1.40546
15 1 5	0.300810	0.300663	0.000147	1.40438	1.40473
22 2 4	0.313810	0.315513	-0.001703	1.37499	1.37127
17 1 5	0.313810	0.315172	-0.001362	1.37499	1.37201
					73

